Mineralization for micropatterned growth of carbonate nanofibers†

Jian-Hua Zhu,[a] Ji-Ming Song,[a] Shu-Hong Yu,*[a] Wei-Qing Zhang[a] and Jin-Xia Shi[b]

Large area arrays of patterned carbonate nanofibers have been constructed *via* polymer controlled mineralization. Micropatterned octadecyltrichlorosilane (OTS)-coated domains on the smooth substrate were found to preferentially deposit mineral films, which could act as a secondary template for growth of nanofibers after their solidification or crystalization.

Bio-inspired synthesis of crystals with complex forms which mimic natural biominerals in the presence of organic template or additives has been developed widely in recent years.[1-4] Among a variety of construction methodologies of functional materials, patterned crystal arrays of organic,[5] inorganic[6] and their hybrid crystals[7] have received considerable attention in recent years for their potential usage in nano-devices.[8] In the past decades, many strategies have been explored to produce crystal arrays. For example, lithography and etching techniques,[9] as a top-down methodology, have been used to pattern many elaborate crystals. Well-defined crystal arrays have been constructed *via* some physicochemical methods such as vapour–liquid–solid (VLS),[10] offering an opportunity for the control of spatial positioning of nanowires. Template-assisted synthesis also provides a general route to replicate the substrate topography, such as close-packed microspheres,[11] producing single crystals with unusual morphologies and patterns.

Recently, self-organized patterns of $CaCO_3$ composites with regular surface-relief structures have been formed from solution on the thin matrix of a hydrophobically modified polysaccharide in the presence of poly(acrylic acid) (PAA).[12] Other feasible routes follow the self-assembled monolayers (SAMs)[13] to create 2D spatially constrained microenvironments for crystallization. Large and patterned single crystal arrays of calcite can be produced by a two-fold strategy involving crystallization of an amorphous calcium carbonate (ACC) precursor phase in a well-defined environment and control of the nucleation event. In this case, crystallization is limited to those microregions that present the appropriate surface property on the substrate. When the patterned substrate is introduced into the mineralization, heterogeneous nucleation for dictating the location and orientation of crystals can be induced.[14] Furthermore, SAMs can shape the transient precursors, such as amorphous calcite carbonate (ACC) or liquid mineral precursor, into complex and ordered structures or arrays.[15]

In this communication, we report a biomimetic approach for patterning carbonate nanofibers. Organic molecular (OTS) was stamped onto the substrate *via* the microcontact printing (μ-CP) technique as a simple analogue of insoluble matrix in biominerals. Different polymers were used to control the crystallization of carbonate. Mineralization process started with the formation of patterned mineral films with smooth and continuous surface as a result of surface modification (Fig. 1a).[16] Interestingly, the mineral films selectively deposited onto the pre-patterned OTS domains, but no mineral films were observed on the glass background. The mineral arrays were soon deposited by some late-formed microspheres (Fig. 1b). On the glass background, the microspheres have a size of 0.9–2.2 μm in diameter (bottom-left inset in Fig. 1b). However, on OTS-coated organic regions, they tend to merge into the former mineral films incompletely and made mineral films bumpy (top-right inset in Fig. 1b). For comparison, hydrophilic glass substrate without OTS coating was used in the experiment and spherical mineral precursor was also observed. The microspheres displayed a fascinating droplet-like shape (ESI, Fig. S3).† Light and polarized microscopic images show that the droplet-like mineral precursor is still in a liquid phase (ESI, Fig. S2a–b).† Prolonged reaction time results in the formation of solidified microspheres which become opaque (ESI, Fig. S2c–d).†

The mineralization seems to go on through a typical polymer-induced liquid-precursor (PILP) process,[17] which is induced by tiny amounts of polyacrylate (PAA, μg mL^{-1} range) in the solution. A special feature of PILP is that it allows easy morphosynthesis of non-equilibrium structures resembling solidified melts (ESI, Fig. S3).† The PILP phase is often produced *via* liquid–liquid phase separation delineated by a virtual phase diagram.[18] In our experiments, the phase separation is observed to take place at different interfaces. When it happens at the liquid/solid interface, the PILP phase will selectively deposit onto the OTS-coated regions (Fig. 1a). Phase separation in

[a] *Division of Nanomaterials and Chemistry, Hefei National Laboratory for Physical Sciences at Microscale, School of Chemistry and Materials, University of Science and Technology of China, Hefei, 230026, P. R. China. E-mail: shyu@ustc.edu.cn; Fax: +0086 551 3603040*
[b] *Department of Polymer and Engineering, University of Science and Technology of China, Hefei, 230026, P. R. China*
† Electronic supplementary information (ESI) available: Additional experimental details. See DOI: 10.1039/b817535g

Fig. 1 SEM image of patterned mineral precursor. (a) Micro-lines of $CaCO_3$ mineral films for 1.5 d. Inset shows the magnified image. (b) Patterned mineral films deposited with mineral droplets for 2 d. Insets show magnified images in different regions (the substrate is coated with micro-lines of OTS molecules on the white areas, at 25 ± 1 °C).

the solution allows the formation of droplet-like microspheres, which suspend in the solution and finally precipitate onto the substrate. Most of them are visible under optical microscopy (ESI, Fig. S2b).† Their random and unselective deposition makes the former patterned mineral films blurred (Fig. 1b), which may have influence on the growth of patterned nanofiber arrays. The experiments show that the nanofibers can not grow from the droplet-like droplets. However, this phenomenon can be avoided if the substrate is placed downward or the mineralization is ceased at an appropriate stage.

The selectivity of ionic mineral precursor onto the OTS-coated surface is unexpected, which could be due to higher roughness of the OTS-stamped films. Atomic force microscopy (AFM) analysis shows that OTS domains exhibit a larger degree of surface roughness (10–14 nm) than the Si background with some OTS "pillars" taller than 100 nm (ESI, Fig. S4).† Mineral ion–substrate interactions are stronger in rough regions of the substrate surface than in the smooth part of the substrate surface.[19] The preferential deposition of mineral films on the OTS-coated domains can be regarded as heterogeneous nucleation. In general, selective nucleation on rough surfaces is in agreement with the classical nucleation theory. Higher surface energy (rough regions) with irregularities such as indentations or protrusions favours heterogeneous nucleation rather than that of a flat surface.[20]

The energy dispersion spectrum (EDS) shows the presence of a Cl element and a high percentage of carbon in the mineral precursor (ESI, Fig. S5),† indicating that the liquid precursor could contain $CaCl_2$, PAA and carbonate ions. The amorphous character of mineral films (for 2 d) can be inferred from the X-ray powder diffraction pattern, which shows no discernible peaks (ESI, Fig. S6a†). The FT-IR spectrum shows a similar result (ESI, Fig. S7a).†

The amorphous mineral films would subsequently transform into a crystalline phase (Fig. 2). After mineralization for 3 d, the patterned mineral films were partially crystallized and only a weak (104) diffraction peak was observed (ESI, Fig. S6b).† After one week, a typical crystalline calcite phase (JCPDS 05-0586) appeared (ESI, Fig. S6c).†
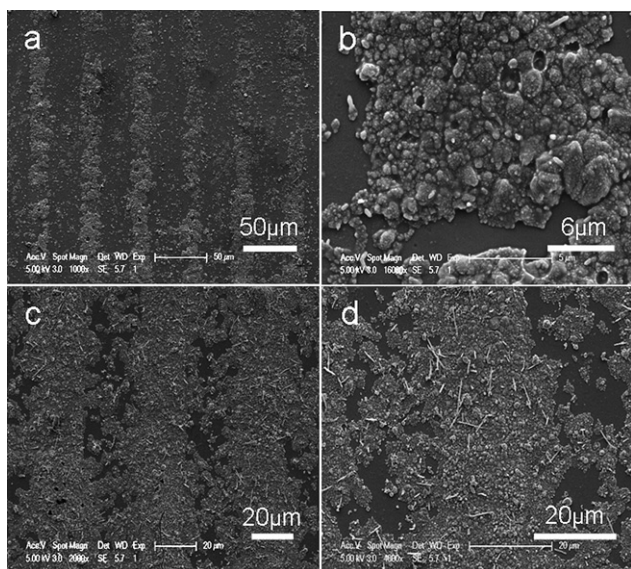
As a new liquid mineral precursor deposited onto the former mineral films, it made the mineral films bumpy with protrusions (Fig. 2b). The most fascinating phenomenon was that new nanorods were observed growing on the mineral films, suggesting that the mineral films could act as a secondary template for the growth of nanofibers. In addition, more nanofibers grew on the mineral films as the transformation process went on (Fig. 2d). The transformation process was initially restricted to the OTS-coated regions (Fig. 2a). Although newly formed mineral films were observed gradually spread into the glass background, few nanofibers were observed (Fig. 2c–d). When mineralization lasted for 5 d, nanofibers and mineral films were observed coexisting on the substrate, but the nanofibers only grew from the mineral films on the substrate decorated with OTS molecules (ESI, Fig. S8a).† The selective growth of nanofibers is a diffusion controlled process, determined by microenvironment around them. As nanofibers initially formed on the OTS-coated region, they will suppress the reagents' diffusion into the environment nearby. Furthermore, if the local reagents in the solution are completely consumed, the solidified mineral films will dissolve back into the solution (ESI, Fig. S8)† and provide an ion reservoir for the continuous growth of nanofibers. Ultimately microlines composed of $CaCO_3$ nanofibers formed after a week (Fig. 3). Nanofibers with diameters ranging from 140–190 nm were long enough to tens of micrometers (Fig. 3b). Most of them lay over the middle of micro-lines. When temperature increased to 25 ± 1 °C, the diameters of nanofibers also increase up to 300 ± 30 nm (Fig. 3c). An interesting feature of the nanofibers is that most of them grow from the underlying crystalline films ever modified with OTS molecules (Fig. 3b), which provides a convenient method for patterned growth of 1D materials on preferential sites of the substrate. That is, different patterns of nanofibers could be obtained *via* changing the location of mineral films on the substrate, whose location is also determined by the pre-printed organic frameworks.

EDS analysis of the $CaCO_3$ nanofiber shows that its atomic ratio of Ca : C : O is close to 1 : 6 : 5 on the tip while in the middle of nanofiber the molar ratio changes into 1 : 2.5 : 3 (ESI, Fig. S9).† A high percentage of C is due to the more PAA adsorbed onto the nanofiber

Fig. 2 SEM images showing the different transformation process of mineral films. (a–b) Gelatinous mineral films with few nanorods, for 3 d; (c–d) mineral films with a few nanofibers, for 4 days (OTS-coated regions are marked by arrows, 25 ± 1 °C).
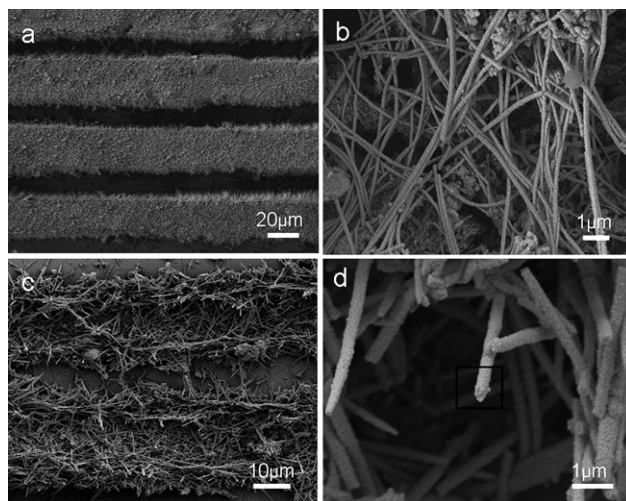
Fig. 3 SEM image of the micropatterns of calcite fibres. (a–d) Micro-lines of calcite nanofibers after mineralization for a week, using substrate modified with micro-lines of OTS molecules; they are obtained at different temperatures: (a–b) 18 ± 1 °C; (c–d) 25 ± 1 °C.

surface, especially on the tips of nanofibers. It indicates that the nanofibers grow *via* the solution–precursor–solid (SPS) process.[21] Tips or "bubbles" of nanofibers play an important role during the growth of nanofibers. A slight amount of PAA diffused into the bubbles will inhibit and delay the crystallization of tips. As new reagents continuously diffuse into them, the tips become solidified (partly crystallized). Newly produced nanoparticles in the growing points will serve as nuclei for the continuous crystallization of the tips. Discontinuous lattice fringes and amorphous nanoregions in the high resolution TEM (HRTEM) image of the nanofiber indicate that its growth is through a typical "mesocrystal" process (Fig. S10†).[22] Vicinal nanoparticles adjust their lattice fringe orientation and fuse together. At last the nanofibers exhibit long-range ordering of nanocrystals owing to vectorially oriented aggregation.[23] A selected-area electron diffractive (SAED) pattern exhibits scattering properties similar to a single crystal. When the nanofibers cease to grow, a slight amount of PAA is occluded into the tips of nanofiber. Droplets-like bubbles are not always observed and they may dissolve back into the solution.

When this synthetic strategy was used into another reaction solution using substrate with different patterns, well-defined micro-squares of $CaCO_3$ and $BaCO_3$ nanofibers have been obtained (Fig. 4). They grow *via* a similar mineralization process as described above (ESI. Fig. S11).† Arrayed $CaCO_3$ nanofibers show a winding and curved morphology. Most of them are tens of micrometers and almost vertical to the substrate. Micro-squares of $BaCO_3$ nanofibers are much shorter than the $CaCO_3$ nanofibers, but their arrays are more regular and can be obtained in a large area (several cm^2).

Similar selective growth of carbonate crystals on the substrate has been reported previously, most of them following the route which uses patterned SAMs on the substrate.[24] What makes our system different is that both nanofibers and the patterned arrays are well controlled and show greater selectivity. In addition, the OTS molecule can be widely used to print other substrates such as oxides and ceramic. As only one molecular "ink" was used for the patterned substrate, this strategy is more convenient to be introduced into other reaction systems.

In summary, a more facile method has been designed for the patterned growth of carbonate nanofibers, *i.e.* a combination of

a microcontact printing technique with a polymer-induced liquid precursor (PILP) process. Selective growth of nanofibers arises from the selective deposition of mineral films, which is due to different roughness of the substrate, and the stronger interaction of the mineral ions with the pre-patterned organic frameworks on the substrate. This biomimetic approach may be expected for patterning growth of other functional inorganic materials.

Notes and references

1 D. B. Deoliveira and R. A. Laursen, *J. Am. Chem. Soc.*, 1997, **119**, 10627.
2 (*a*) T. Kato, A. Sugawara and N. Hosoda, *Adv. Mater.*, 2002, **14**, 869; (*b*) H. Cölfen and S. Mann, *Angew. Chem., Int. Ed.*, 2003, **42**, 2350.
3 (*a*) For reviews see S. H. Yu and H. Cölfen, *J. Mater. Chem.*, 2004, **14**, 2124, and references therein; (*b*) H. Cölfen and S. H. Yu, *MRS Bull.*, 2005, **30**, 727, and references therein.
4 G. Falini, S. Albeck and L. Addadi, *Science*, 1996, **271**, 67.
5 D. D. Sawall, R. M. Villahermosa, R. A. Lipeles and A. R. Hopkins, *Chem. Mater.*, 2004, **16**, 1606.
6 (*a*) S. A. Morin, F. F. Amos and S. Jin, *J. Am. Chem. Soc.*, 2007, **129**, 1377; (*b*) T. X. Wang, A. Reinecke and H. Cölfen, *Langmuir*, 2006, **22**, 8986.
7 (*a*) S. Tugulu, M. Harms, M. Fricke, D. Volkmer and H. A. Klok, *Angew. Chem., Int. Ed.*, 2006, **45**, 7458; (*b*) S. Ludwigs, U. Steiner, A. N. Kulak, R. Lam and F. C. Meldrum, *Adv. Mater.*, 2006, **18**, 2270.
8 A. L. Briseno, S. B. Mannsfeld, M. M. Ling, S. H. Liu, J. R. Tseng, C. Reese1, M. E. Roberts, Y. Yang, F. Wudl and Z. N. Bao, *Nature*, 2006, **444**, 913.
9 (*a*) B. D. Gates, Q. B. Xu, M. Stewart, D. Ryan, C. G. Willson and G. M. Whitesides, *Chem. Rev.*, 2005, **105**, 1171; (*b*) C. H. Lu, L. M. Qi, J. M. Ma, M. F. Zhang and W. X. Cao, *Langmuir*, 2004, **20**, 7378.
10 M. H. Huang, Y. Y. Wu, H. Feick, N. Tran, E. Weber and P. D. Yang, *Adv. Mater.*, 2001, **13**, 113.
11 F. C. Meldrum and S. Ludwigs, *Macromol. Biosci.*, 2007, **7**, 152.
12 (*a*) A. Sugawara, T. Ishii and T. Kato, *Angew. Chem., Int. Ed.*, 2003, **42**, 5299; (*b*) T. Satamoto, A. Oichi, A. Sugawara and T. Kato, *Chem. Lett.*, 2006, **35**, 310.
13 J. Aizenberg, *Adv. Mater.*, 2004, **16**, 1295.
14 J. Aizenberg, D. A. Muller, J. L. Grazul and D. R. Hamann, *Science*, 2003, **299**, 1205.
15 (*a*) E. Loste and F. C. Meldrum, *Chem. Commun.*, 2001, **10**, 901; (*b*) E. Loste, R. J. Park, L. Warren and F. C. Meldrum, *Adv. Funct. Mater.*, 2004, **14**, 1211; (*c*) Y. Y. Kim, E. P. Douglas and L. B. Gower, *Langmuir*, 2007, **23**, 4862.
16 Y. Y. Kim and L. B. Gower, *Mater. Res. Soc. Symp. Proc.*, 2002, **724**, 941.
17 (*a*) S. Wohlrab, H. Cölften and M. Antonietti, *Angew. Chem., Int. Ed.*, 2005, **44**, 4087; (*b*) L. B. Gower and D. J. Odom, *J. Cryst. Growth*, 2000, **210**, 719.
18 M. Faatz, F. Gröhn and G. Wegner, *Adv. Mater.*, 2004, **16**, 996.
19 S. B. Mannsfeld, A. L. Briseno, S. H. Liu, C. Reese, M. E. Roberts and Z. N. Bao, *Adv. Funct. Mater.*, 2007, **17**, 3545.
20 (*a*) L. Addadi, S. Raz and S. Weiner, *Adv. Mater.*, 2003, **15**, 959; (*b*) J. Aizenberg, D. A. Muller, J. L. Crazul and D. R. Hamann, *Science*, 2003, **299**, 1205; (*c*) G. Xu, N. Yao, I. A. Akasay and J. T. Groves, *J. Am. Chem. Soc.*, 1998, **120**, 11977.
21 M. J. Olszta, S. Gajjeraman, M. Kaufman and L. B. Gower, *Chem. Mater.*, 2004, **16**, 2355.
22 (*a*) H. Cölfen and M. Antonietti, *Angew. Chem., Int. Ed.*, 2005, **44**, 5576; (*b*) T. X. Wang, H. Cölfen and M. Antonietti, *J. Am. Chem. Soc.*, 2005, **127**, 3246.
23 J. H. Zhu, S. H. Yu, A. W. Xu and H. Cölfen, *Chem. Commun.*, 2009, DOI: 10.1039/B817048G.
24 Y. Y. Kim and L. B. Gower, *Mater. Res. Soc. Symp. Proc.*, 2003, **774**, 141.
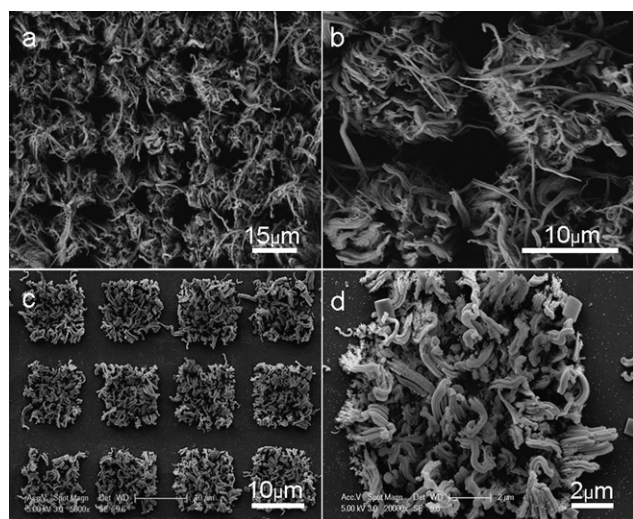
Fig. 4 SEM images of well-defined micro-squares composed of (a–b) $CaCO_3$ nanofibers, 7 days (c–d) $BaCO_3$ nanofibers, for 3 days.